Cloaking Against Thermal Imaging

Maple So
Rose-Hulman Institute of Technology
Mathematics Research Experience for Undergraduates Program

November 4, 2011

Abstract

There has been a lot of recent interest in cloaking and invisibility in the mathematics and science communities, and in fact physically plausible mechanisms have been proposed (some built) for cloaking an object against detection using a variety of electromagnetic methods. The ideas are very general, however, and should allow one to design cloaks that work against other forms of imaging. We examine the possibility of cloaking an object to make it invisible to an observer using thermal energy (heat) as the imaging tool. Specifically, we desire to cloak an object inside a two-dimensional disk by cutting a small hole in the center of the disk in which to place the particular object. Mathematically, we want to make a large cavity in the unit disk to appear small to outside observers. This involves analysis the solution to a PDE and the solution behavior under a change-of-variables argument.

1 Introduction

Cloaking has attracted the attention of multiple fields in science and technology. The idea of cloaking is to render an object invisible to outside observers. Several examples of cloaking arise in modern science fiction and fantasy, such as, Harry Potter's invisibility cloak and the Romulan ships from the "Star Trek" series [2]. Generally speaking, one wants to hide an object from outsiders so that they will not even notice the hidden object.

1.1 Basic Idea

To illustrate the basic idea of cloaking, imagine the unit disk in two-dimensional space as displayed in Figure 1. On the outer edge of the disk, an observer shines a flashlight across the interior while examining the beam of light on the other end of the disk. If the disk does not contain any hidden objects in the center, then the beam of light will shine across the disk without interruption. Hence, the observer will see the undisturbed beam of light coming from the other end. Next, we describe the case of bad cloaking. One hides an object by simply placing the object in the center of the unit disk. The outsider will shine a beam of

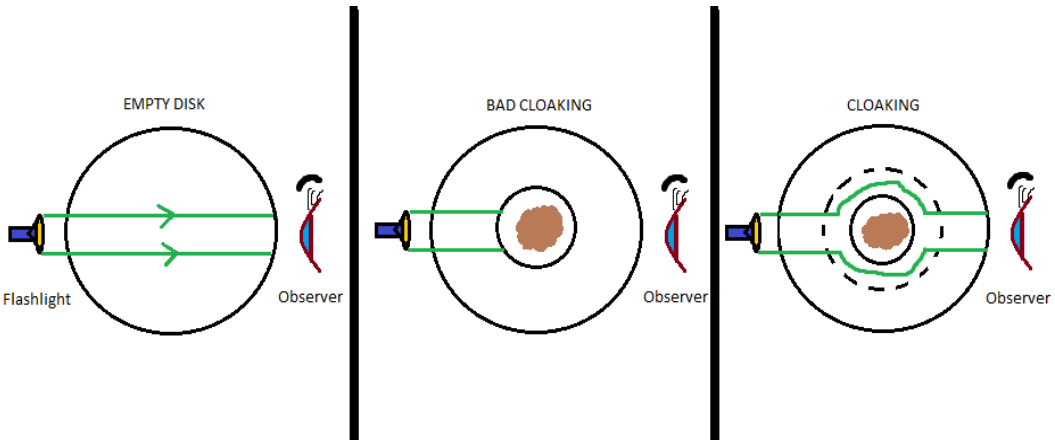

Figure 1: *This diagram explains the differences between the empty disk, "bad" cloaking and good cloaking. The disk with no cloaking shows the beams of light shining across the empty disk without interruption, as the observer watches the receiving beams on the other end of the disk. The disk in the middle illustrates the idea of bad cloaking (really, no cloaking) with the hidden object placed in the center of disk. Note that the path of the light beam gets interrupted by the object in the middle. On the far right, enhanced cloaking utilizes a special wrapping that bends the light rays around the hidden object so the observer cannot find any notable differences between the receiving light beams on the ends of the empty disk when compared to the disk with the hidden object.*

light and notice the interruption in the center of the disk as the light beam attempts to make its way across the other end of the disk. Although the observer may not know what the disk hides, he becomes aware of the suspicious activity. This is analogous to wrapping a gift; the observer may not know what is hidden, but he notices that something is hidden. Ideally, one can wrap the object with an artificial material with the special property of bending light in the desired direction so the observer will see the receiving beams as if no interruptions occurred. This is the case of good cloaking as illustrated by the third diagram in Figure 1.

2 Previous Work in Cloaking

An expository article by Kurt Bryan and Tanya Leise in 2010 for cloaking against electrical impedance tomography motivated the idea of cloaking against thermal energy. In this section, we explain briefly explain electrical impedance tomography (EIT), an imaging technique based on input electrical currents and measured voltages. We briefly discuss and outline prior results in cloaking against this form of imaging and the mathematics behind designing good cloaks against EIT. This involves a change-of-variables argument and leads to the notion of a "metamaterial." In the next section we apply these techniques, and supply more details, to show how to cloak against thermal energy.

2.1 Electrical Impedance Tomography

Suppose an observer attempts to image the interior of an unknown region or domain by sending some input energy into the regions and measuring outputs. Based on the output data, the observer forms an educated guess about the interior. Electrical impedance tomography (EIT) is one such imaging technique that has already found application in the medical field. In EIT one injects electrical current on the outer boundary of a region through attached electrodes and then measures the voltages induced as current flows, to generate an image of the interior electrical conductivity of the object. Organs have varying conductivity, so they appear as different colors as shown in Figure 2. Regions with high conductivity are shown in red, while regions with lower conductivity are shown in blue. The specific algorithms that allow the reconstruction of images from boundary data are not at the moment important to the discussion.

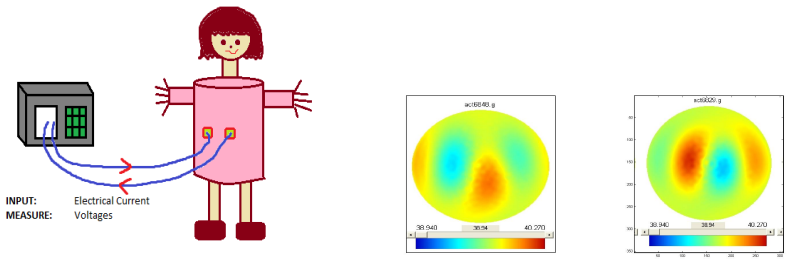

Figure 2: *A specific use of electrical impedance tomography is in medical imaging. A patient has electrodes adhered onto her torso as the machine on the left emits electrical current into her body while taking voltage measurements. We acknowledge David Isaacson and the Electrical Impedance Imaging group at the Rensselaer Polytechnic Institute for their contribution of the torso images from their ACT III impedance imaging system [2].*

In the next couple subsections we show how to model the conduction of electrical current through an object, how this can be used (in a very simple context) to form an image of the interior of an object, and then lead up to a description of techniques that have been developed to cloak against this form of imaging. Our ultimate goal is to cloak against any sort of imaging that uses energy to collect information about the concealed object, though we focus on the case of thermal imaging.

2.2 Conductivity

The artificial material required for cloaking has the special property of bending light or other forms of energy in a controllable way and is known as a *metamaterial*. In order to evade the observer's detection, a metamaterial guides the incoming rays in the ideal direction as shown by the green beams in the yellow region in Figure 3. In the context of EIT this requires that the material have an anisotropic conductivity.

In what follows we consider a model for electrical conduction through an object Ω. The two types of conductivity with which we will be concerned are *isotropic and anisotropic*. Let $\vec{J}$ denote the electric current flux in Ω and $\vec{E}$ be the electric field. If a given material

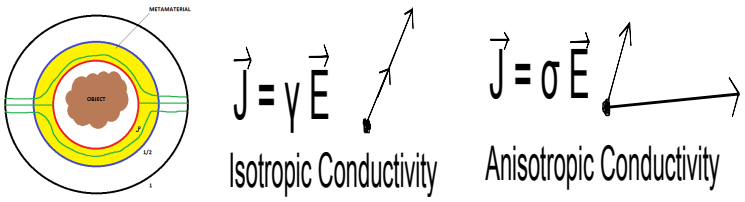

Figure 3: *Anisotropic conductivity is needed in the metamaterial as shown in the yellow region.*

has isotropic conductivity, then $\vec{J} = \gamma\vec{E}$, where γ is a positive scalar, or scalar function of position. In isotropic conduction the current flows in the direction of the electric field, so $\vec{J}$ and $\vec{E}$ are parallel. In the metamaterial used for cloaking the conductivity must also have directional properties, so that it can guide the incoming electric current in the proper direction. An anisotropic conductivity σ yields $\vec{J} = \sigma\vec{E}$, where σ is a 2-by-2 symmetric positive definite matrix. In this case $\vec{E}$ and $\vec{J}$ need not be parallel. However, $\vec{E}$ and $\vec{J}$ will lie within 90 degrees of each other, since

$$\vec{J} \cdot \vec{E} = \vec{J}^T\vec{E} = (\vec{E}\sigma)^T\vec{E} = \vec{E}^T\sigma^T\vec{E} > 0$$

if $\vec{E} \neq \vec{0}$, since σ is positive definite.

2.3 Defining the Domains

In order to clearly describe the mathematics in cloaking, we utilize two domains throughout the paper. We compare the two domains needed in cloaking against outer detection: the unit disk Ω_0 and the annulus Ω_ρ. Figure 4 clearly illustrates the two domains of interest.

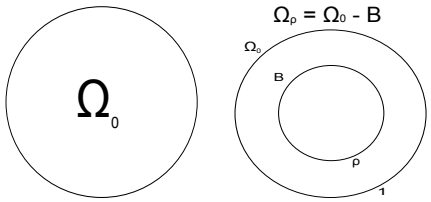

Figure 4: *The unit disk and the annulus used in cloaking.*

We refer to Ω_0 as the "empty" unit disk. We shall denote the boundary of the empty disk by $\partial\Omega_0$. Let $u_0(x, y)$ be the electric potential on Ω_0 where (x, y) represents the Cartesian coordinates. On the boundary $\partial\Omega_0$, we impose boundary condition $u_0 = f$, where f is the input Dirichlet data chosen by the observer. The observer measures the output data, the electric current flux $\frac{\partial u_0}{\partial n}$ on $\partial\Omega_0$ (a Neumann boundary condition), to acquire information about the interior of the disk. The Dirichlet-Neumann data pair encodes some information about the interior electrical conductivity of Ω_0.

Let $\Omega_\rho = \Omega_0 \setminus B_\rho$ represent the annulus, where B_ρ denotes the inner hole of radius ρ, where $0 < \rho < 1$. We shall denote the outer boundary of the annulus by $\partial\Omega_\rho$ and the inner boundary of the annulus by ∂B_ρ. Similarly, let $u_\rho(x, y)$ be the potential on Ω_ρ where (x, y)

represents the Cartesian coordinates. On the outer boundary $\partial\Omega_\rho$, we have boundary condition $u_\rho = f$ with f being some chosen boundary potential from the observer. Similarly, the observer gathers output data, $\frac{\partial u_\rho}{\partial n}$, to obtain information about the interior of the annulus. On the inner boundary, ∂B we assume $\frac{\partial u_\rho}{\partial n} = 0$, that is, the inner boundary is electrically insulating.

2.4 Prior Work

Based on previous researchers, extensive mathematical work has been done on cloaking against EIT. In the electrical case, consider the region Ω_0, and suppose we have isotropic conductivity. Recall that $\vec{J}$ is the electric current and $\vec{E}$ represents the electric field on the unit disk. Thus, the following equation must be satisfied [2]. We then have

$$\vec{J} = \gamma\vec{E}$$

By conservation of charge, we have $\nabla \cdot \vec{J} = 0$, so that in the region Ω_0

$$\nabla \cdot \gamma\nabla u_0 = 0.$$

If γ is constant, as we now assume, this can be simplified to Laplace's equation

$$\frac{\partial^2 u_0}{\partial x^2} + \frac{\partial^2 u_0}{\partial y^2} = \Delta u_0 = 0.$$

On the boundary $\partial\Omega_0$, we have imposed Dirichlet condition

$$u_0 = f$$

By s standard method in separation of variables in polar coordinates we get the following solution for Laplace's Equation on the unit disk:

$$u_0(r,\theta) = A_0 + \sum_{k\in\mathbb{Z}\setminus\{0\}} (A_k r^{|k|} + B_k r^{-|k|})e^{ik\theta}$$

where the A_k and B_k are coefficients that can be found from the boundary data f; see [2].

We can also compute the solution to Laplace's Equation on the annulus Ω_ρ with $u_\rho = f$ on the outer boundary and Neumann boundary condition $\frac{\partial u_\rho}{\partial n} = 0$ on ∂B. Using similar separation of variables and a change to the polar coordinate system, we obtain

$$u_\rho(r,\theta) = C_0 + D_0\ln(r) + \sum_{k\in\mathbb{Z}\setminus\{0\}} (C_k r^{|k|} + D_k r^{-|k|})e^{ik\theta}$$

where u_ρ is the voltage on Ω_ρ. The C_k and D_k can be found from the boundary data f; again, see [2].

At this point, it is not vital to compute the values of the Fourier coefficients. We merely note that the difference between the Neumann boundary data on the unit disk and the

annulus is small as $\rho \to 0$. Indeed, in [2] it is shown that the L^2 norm of the difference $\frac{\partial u_\rho}{\partial n} - \frac{\partial u_0}{\partial n}$ on the boundary of the disk $r = 1$ is bounded by the L^2 norm of the Neumann data on $\partial\Omega_0$ times ρ^2. That is,

$$\left\| \frac{\partial u_0}{\partial n} - \frac{\partial u_\rho}{\partial n} \right\|_2 \leq C\rho^2 \tag{1}$$

for some constant C (independent of ρ), where $\|\cdot\|_2$ is the usual $L^2(\partial\Omega_0)$ norm. This means that as $\rho \to 0$ the difference in the Neumann data between the disk and the annulus is close to zero. This makes intuitive sense: small holes ($\rho \approx 0$) cause little disruption in the electric potential. Thus, the observer may not detect any differences in the Neumann data between the two regions, provided that ρ is sufficiently small (and the observer makes measurements of the Neumann data at finite precision).

This fact is essential to showing that cloaking works, which we now describe.

2.5 Cloaking on an Annulus

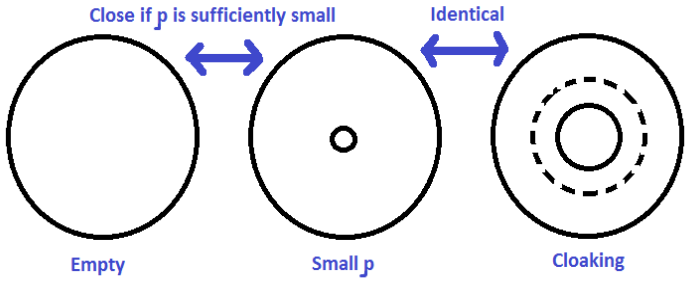

Figure 5: *Here is an intuitive diagram of how we want to cloak on an annulus. Ideally, we desire to make a large hole look very small.*

In order to render an object invisible to outsiders, the inner hole of radius ρ must be sufficiently small to avoid detection. However, technical challenges arises if ρ is too small because hiding objects in a very small region may not be physically possible. Therefore, we attempt to mask a large hole look like a small hole to an observer. Let's suppose we want to the inner ball $B = B_a$ to have radius "a", where a is large, say $a = 1/2$. This gives us room to hide a large object inside B_a; unfortunately, such a large hole is easily detectable with EIT. We will show how to use an anisotropic conductor (physically, a metamaterial) to make B_a appear as a hole of radius $\rho \approx 0$ to an outside observer using EIT. By transitivity, the annulus with inner radius a will then be hard to distinguish from the empty disk Ω_0.

Figure 5 shows an intuitive diagram of making a large hole appear small. The cloaking will be performed on the annulus with radius a by surrounding the inner hole with a meta-material as denoted by the dotted line inside the third disk in the drawing. As detailed in the previous section we have the estimate (1). This means that when the observer inputs Dirichlet data f onto the boundary of Ω_0 and Ω_ρ, the output data will be close together such

that their differences is small. Hence, the observer taking finite precision data may conclude that an annulus with a very small inner radius is an empty unit disk.

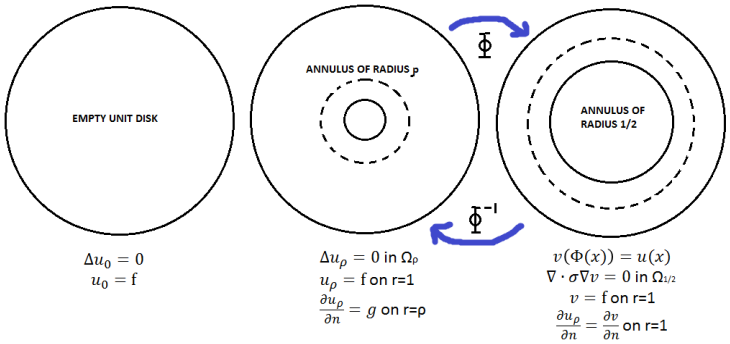

Figure 6: *The diagram illustrates the idea of cloaking against electrical impedance tomography.*

In order to construct the cloak, one can use a change-of-variables argument as detailed in [2]. Briefly, we map the domain Ω_ρ (central hole of radius ρ) to the domain $\Omega_{1/2}$ (large center hole of radius $1/2$) with an invertible mapping Φ. This mapping is purely radial, maps the boundary of B_ρ (a circle of radius ρ) to the circle of radius $1/2$, and fixes a neighborhood of the outer boundary $\partial\Omega_0$. We define a "pushed forward" function v_ρ via the relation $v_\rho(\mathbf{y}) = u_\rho(\mathbf{x})$ where $\mathbf{y} = \Phi(\mathbf{x})$. The $\mathbf{x}$ coordinates represent the Cartesian coordinates on Ω_ρ, and the $\mathbf{y}$ coordinates represent the Cartesian coordinates on $\Omega_{\frac{1}{2}}$. Figure 6 gives an intuitive illustration of cloaking a large hole in impedance imaging. The central result of interest is the following lemma, proved in [2]. A variation and proof of this for thermal energy is given later in this paper.

Lemma 1 *Under the assumptions above the function $v(\mathbf{y})$ satisfies the partial differential equation*

$$\nabla \cdot \sigma(\mathbf{y}) \nabla v = 0$$

in $\Omega_{\frac{1}{2}}$, where $\sigma(\mathbf{y})$ denotes the 2x2 matrix

$$\sigma(\mathbf{y}) = \frac{D\Phi(\mathbf{x})(D\Phi(\mathbf{x}))^T}{|det(D\Phi(\mathbf{x})|}$$

with

$$D\Phi(x) = \begin{bmatrix} \frac{\partial y_1}{\partial x_1} & \frac{\partial y_1}{\partial x_2} \\ \frac{\partial y_2}{\partial x_1} & \frac{\partial y_2}{\partial x_2} \end{bmatrix}$$

evaluated at $x = \Phi^{-1}(\mathbf{y})$.

In the dashed region on the subfigure on the right in Figure 6 the matrix σ can be interpreted as an anisotropic conductivity.

This change-of-variables argument will be further discussed and extended in cloaking against thermal imaging.

3 Transition to Thermal Energy

Similar to cloaking against impedance imaging, we will show how to cloak against an observer using thermal energy. The idea is the same: make a large hole appear like a small hole by wrapping the large hole with a layer of metamaterial. We will derive the required properties of the metamaterial in the change-of-variables argument for the heat equation. Additionally, we will show that the annulus with inner radius $\rho \approx$ looks like the unit disk to an observer using heat, provided that ρ is small.

We use $u(x, y, t)$ to denote the time-varying temperature of a region in the plane. Let us suppose that the region has density ρ, dimensions mass per area, specific heat c of dimensions energy per degree per mass, and isotropic thermal conductivity γ; each of c, ρ, and γ may depend on position. The usual model of heat conduction is

$$cp\frac{\partial u}{\partial t} - \gamma \Delta u = 0. \tag{2}$$

If the material has anisotropic thermal conductivity the model is

$$cp\frac{\partial u}{\partial t} - \sigma \Delta u = 0. \tag{3}$$

As in the case of impedance, σ is a 2×2 positive definite matrix. The Laplacian of u is being applied only to the spatial xy-coordinates.

The essential constitutive relation underlying equation (2) is $\vec{J} = -\gamma \nabla u$, where $\vec{J}$ is the heat flux; that is, we assume in the isotropic case that heat flows downhill in the steepest possible direction $(-\nabla u)$. For the anisotropic case we assume $\vec{J} = -\gamma \nabla u$. Since $\vec{J}$ is in the negative direction of the gradient of u, then this implies that the thermal flux goes from hotter temperatures to colder temperatures.

3.1 Periodic Heat Equation

Prior work has been done on Laplace's Equation with specific application in the electrical case; we now attempt to cloak against thermal energy instead of electrical current. To simplify matters, we will assume that the temperature $u(x, y, t)$ is periodic in time. This allows us to adapt the techniques for EIT cloaking more easily.

In the periodic heat equation we assume the solution $u_0(x, y, t)$ (temperature) is of the form

$$u_0(x, y, t) = w(x, y)e^{i\omega t} \tag{4}$$

for some function $w(x, y)$ and fixed frequency $\omega > 0$. If we insert u_0 into the heat equation (2) and simplify we obtain

$$icp\omega w - \gamma \Delta w = 0 \tag{5}$$

for the isotropic conduction and

$$icp\omega w - \nabla \cdot \sigma \nabla w = 0 \tag{6}$$

for the anisotropic conduction.

3.1.1 Periodic Heat Equation on the Unit Disk and Annulus

Let's consider the case in which Ω_0 is the unit disk. We will consider equation (5) in the case $c = \rho = \gamma = 1$. We also suppose that an input heat flux $g(x, y)$ is imposed on $\partial\Omega_0$ (corresponding to an input heat flux $g(x, y)e^{i\omega t}$ in the full time-dependent case). With $w_0(x, y)$ as the spatial part of the solution we obtain

$$\begin{aligned} \triangle w_0 - iw_0 &= 0 \text{ in } \Omega_0 \quad (7) \\ \frac{\partial w_0}{\partial n} &= g \text{ on } \partial\Omega_0. \quad (8) \end{aligned}$$

Equation (7) can be solved in polar coordinates via separation of variables. Equation (7) becomes

$$\frac{\partial^2 w_0}{\partial r^2} + \frac{1}{r}\frac{\partial w_0}{\partial r} + \frac{\partial^2 w_0}{\partial \theta^2}\frac{1}{r^2} = i\omega w_0. \quad (9)$$

Suppose $w_0(r, \theta) = R(r)\Theta(\theta)$. We find, after a standard separation argument, that $\Theta(\theta) = e^{ik\theta}$ and

$$R''(r) + \frac{R'(r)}{r} - R(r)(i\omega + \frac{k^2}{r^2}) = 0, \quad (10)$$

where $k \in \mathbb{Z}$ represents the eigenvalues to the differential equation. Equation (10) is known as the *Modified Bessel's Differential Equation* (see [3], [4]). The solution is is any linear combination of the modified Bessel functions I_k and K_k (see [5]),

$$R_k(r) = C_k I_k(-i\sqrt{-i\omega}r) + D_k K_k(-i\sqrt{-i\omega}r). \quad (11)$$

Here C_k and D_k are arbitrary constants. The function $I_k(-i\sqrt{-i\omega}r)$ is the *Modified Bessel Function of the First Kind* and $K_k(-i\sqrt{-i\omega}r)$ is the *Modified Bessel Function of the Second Kind*. Mathematically, the $K_k(-i\sqrt{-i\omega}r)$ must be excluded in $R(r)$ because it is not bounded as $r \to 0$ (see [4]).

The full solution for w_0 on the unit disk Ω_0 is thus

$$w_0(r, \theta) = \sum_{k=-\infty}^{\infty} C_k I_k(-i\sqrt{-i\omega}r)e^{ik\theta} \quad (12)$$

where the constants C_k can be determined from the Neumann boundary condition (8).

On the annulus Ω_ρ the periodic heat equation becomes

$$\begin{aligned} \triangle w_\rho - iw_\rho &= 0 \text{ in } \Omega_\rho \quad (13) \\ \frac{\partial w_\rho}{\partial n} &= g \text{ on } \partial\Omega_0. \quad (14) \\ \frac{\partial w_\rho}{\partial n} &= 0 \text{ on } \partial B_\rho \quad (15) \end{aligned}$$

where w_ρ is the spatial portion of the solution. Note we model the boundary of the region ∂B_ρ (just the circle $r = \rho$) as being a perfect thermal insulator via equation (15).

A very similar analysis on the annulus Ω_ρ yields a solution of the form

$$w_\rho(r, \theta) = \sum_{k=-\infty}^{\infty} (C_k I_k(-i\sqrt{-i\omega}r) + D_k K_k(-i\sqrt{-i\omega}r))e^{ik\theta} \quad (16)$$

where, since $r > \rho$, the function K_k can (indeed must) be included. The constants C_k and D_k can be found from the boundary conditions (14) and (15).

We will in fact not pursue the necessary cloaking results, in particular, estimates on the size of $w_\rho - w_0$, using these expressions for the solutions—the analysis turns out to be somewhat difficult. Instead, in section **??** we use somewhat more abstract arguments to make the necessary estimates.

3.2 Change-of-Variables Argument

As mentioned, we will cloak an interior ball of large radius, e.g., 1/2, by wrapping it with a suitable layer of an anisotropic thermal conductor. The properties we need for this anisotropic conductor can be deduced from a simple change-of-variables argument involving the PDE (5). Let Ω_ρ be the annulus with a hole of radius ρ and Ω_a be the annulus with a hole of radius a, where $\rho < a < 1$. We arbitrarily choose $a = \frac{1}{2}$ in the rest of our argument.

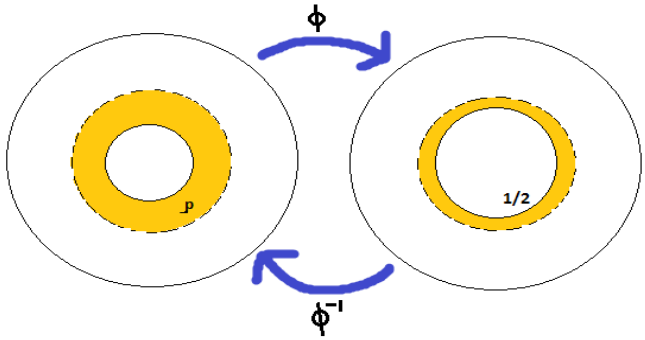

Figure 7: *The diagram above shows the change of variables needed in cloaking a large hole to a small hole by using an invertible mapping* Φ.

Define a mapping $\Phi : \Omega_\rho \to \Omega_{\frac{1}{2}}$ to be an invertible map that of the general form indicated in Figure 7. In particular, we need that Φ maps $r = \rho$ to $r = 1/2$, and that Φ fixes the region $1/2 + \delta < r < 1$ for some $\delta \in (0, 1/2)$. We want Φ, and Φ^{-1}, to be twice continuously differentiable on the closure of their domains. We may take Φ to be purely radial as well. Many such mappings can be written down, but the precise form is unimportant at the moment.

3.2.1 Change of Variables for the Periodic Heat Equation

Let $\mathbf{x} = (x_1, x_2)$ be the Cartesian coordinates for the region Ω_ρ, and $\mathbf{y} = (y_1, y_2)$ be the Cartesian coordinates for the region $\Omega_{\frac{1}{2}}$. We use w_ρ for the solution to (7). Let $z(\mathbf{y})$ be the function w_ρ pushed forward from Ω_ρ onto $\Omega_{\frac{1}{2}}$ by the transformation Φ, so $z(\Phi(\mathbf{x})) = w_\rho(\mathbf{x})$, or $z(\mathbf{y}) = w_\rho(\Phi^{-1}(\mathbf{y}))$. The following is a generalization of Lemma 3.1 in [2].

Lemma 2 *Let $z(\mathbf{y})$ be as stated above. Then z satisfies the PDE*

$$\nabla \cdot \sigma(\mathbf{y}) \nabla z - \frac{i\omega z}{|\det(D\Phi)|} = 0 \tag{17}$$

in $\Omega_{\frac{1}{2}}$, where $\sigma(\mathbf{y})$ is the 2x2 matrix

$$\sigma(y) = \frac{D\phi(\mathbf{x})(D\phi(\mathbf{x}))^T}{|\det(D\phi)|} \tag{18}$$

evaluated at $\mathbf{x} = \phi^{-1}(\mathbf{y})$.

Proof: Let $s(\mathbf{x})$ be an arbitrary continuously differentiable function defined on Ω_ρ with $s = 0$ on $\partial\Omega_\rho$, and define $\tilde{s}(\mathbf{x})$ on $\Omega_{\frac{1}{2}}$ by $s(\mathbf{x}) = \tilde{s}(\Phi(\mathbf{x}))$. We thus have

$$\int_{\Omega_\rho} s(\mathbf{x})(\Delta_x w_\rho - i\omega u s(\mathbf{x}))dx = 0 \tag{19}$$

where Δ_x means the Laplacian applied in the $\mathbf{x}$ variable.

Making use of the vector identity $s\Delta_x w_\rho = \nabla_x \cdot (s\nabla_x w_\rho) - \nabla_x s \cdot \nabla_x w_\rho$ in (19) yields

$$\int_{\Omega_\rho} \nabla_x \cdot (s\nabla_x w_\rho) - \nabla_x s \cdot \nabla_x w_\rho - i\omega w_\rho s(\mathbf{x})dx = 0. \tag{20}$$

The Divergence Theorem shows that

$$\textstyle\int_{\Omega_\rho} \nabla_x \cdot (s\nabla_x w_\rho) = \int_{\partial\Omega_\rho} s(\mathbf{x})\nabla_x w_\rho \cdot n \; ds.$$

Since $s = 0$ on $\partial\Omega_\rho$ both sides above are zero and equation (20) becomes

$$\int_{\Omega_\rho} (\nabla_x s \cdot \nabla_x w_\rho + si\omega w_\rho)dx = 0. \tag{21}$$

Now we have $\nabla_x s \cdot \nabla_x w_\rho = \nabla_x s^T \nabla_x w_\rho$, and from the chain rule

$$\begin{aligned} \nabla_x w_\rho &= (D\Phi(\mathbf{x}))^T \nabla_y z(\Phi(\mathbf{x})) \\ \nabla_x s &= (D\Phi(\mathbf{x}))^T \nabla_y \tilde{s}(\Phi(\mathbf{x})) \end{aligned}$$

where $\tilde{s}(\mathbf{y}) = s(\mathbf{x})$ is the function s in the $\mathbf{y}$ coordinates on $\Omega_{1/2}$. Equation (21) now becomes

$$\textstyle\int_{\Omega_\rho} \nabla_y \tilde{s}(\Phi(\mathbf{x}))^T D\Phi(\mathbf{x})(D\Phi(\mathbf{x}))^T \nabla_y z(\Phi(\mathbf{x})) + i\omega s w_\rho \; dx = 0$$

We now make a change of variable in the integral, to the $\mathbf{y}$ coordinate system on $\Omega_{1/2}$, noting that $d\mathbf{x} = d\mathbf{y}/|\det(D\Phi)|$. We obtain

$$\int_{\Omega_{1/2}} \nabla_y \tilde{s}(\mathbf{y})^T (\sigma(\mathbf{y})\nabla_y z(\mathbf{y})) + \frac{\tilde{s}(\mathbf{y}) i\omega z(\mathbf{y})}{|\det(D\Phi)|} \; dy = 0 \tag{22}$$

where $\sigma(y)$ is as in the statement of the lemma.

An straightforward vector calculus computation shows that

$$\nabla_y \tilde{s}\mathbf{y})^T(\sigma(\mathbf{y})\nabla_y z(\mathbf{y}) \;\; = \;\; \nabla_y \cdot (\tilde{s}(\mathbf{y})^T\sigma(\mathbf{y})\nabla_y z(\mathbf{y})) - \tilde{s}(\mathbf{y})\nabla_y \cdot (\sigma(\mathbf{y})\nabla_y z(\mathbf{y}))$$

If we make use of this in (22) we find

$$\int_{\Omega_{1/2}} \nabla_y \cdot (\tilde{s}(\mathbf{y})\sigma(\mathbf{y})\nabla_y z(\mathbf{y})) - \tilde{s}(\mathbf{y})\nabla_y \cdot (\sigma(\mathbf{y})\nabla_y z(\mathbf{y})) + \frac{\tilde{s}(\mathbf{y})i\omega z(\mathbf{y})}{|\det(D\Phi)|}\, dy = 0. \tag{23}$$

However, by the Divergence Theorem we have

$$\int_{\Omega_{1/2}} \nabla_y \cdot (\tilde{s}(\mathbf{y})\sigma(\mathbf{y})\nabla_y z(\mathbf{y}))\, dy = \int_{\partial\Omega_{1/2}} (\tilde{s}(\mathbf{y})(\sigma(\mathbf{y})\nabla_y z(\mathbf{y}))) \cdot n\, ds_y = 0$$

because $\tilde{s} = 0$ on $\partial\Omega_{1/2}$. Equation (23) then becomes

$$\int_{\Omega_{\frac{1}{2}}} \tilde{s}(\mathbf{y}) \left[-\nabla_y \cdot (\sigma(\mathbf{y})\nabla_y z(\mathbf{y})) + \frac{i\omega z(\mathbf{y})}{|\det(D\Phi)|} \right]\, dy = 0. \tag{24}$$

Because equation (24) holds for an arbitrary function $\tilde{s}(\mathbf{y})$ we must conclude that

$$-\nabla_y \cdot (\sigma(y)\nabla_y z(y)) + \frac{i\omega z(y)}{|\det(D\Phi)|} = 0$$

in $\Omega_{1/2}$. This completes the proof of the lemma.

3.2.2 Physical Implication

In order to interpret the physical meaning of equation (17) let us examine the equation heat equation for anisotropic conductivity, namely

$$cp\frac{\partial u}{\partial t} - \nabla \cdot (\sigma \nabla u) = 0, \tag{25}$$

where as mentioned above c is the specific heat, p is the density (2D) and σ is the thermal conductivity. The spatial part of a time-periodic solution to (25) would satisfy the PDE (6). Comparison of (6) and (17) shows that we may make the identification $cp = 1/|\det(D\Phi)|$, while the matrix σ in (17) may be interpreted as an anisotropic thermal conductivity. However, unlike the impedance imaging case, we must now change the material properties of the region—the quantity cp—order to cloak. Lemma 2 then shows that under these conditions, any solution to

$$\triangle w_\rho - i\omega w_\rho = 0$$

with insulating conditions on $r = \rho$ will have a corresponding solution to (17) on $\Omega_{1/2}$ with EXACTLY the same Cauchy (Dirichlet and Neumman) data. In other words, the two internal structures are indistinguishable with this type of imaging.

It's interesting to examine the quantity cp under a typical change of variable. We follow the specific example from ([2]) with $\Phi(\mathbf{x}) = \frac{\Psi(||\mathbf{x}||)}{||\mathbf{x}||}\mathbf{x}$, where $\Psi(||\mathbf{x}||)$ must be a twice, continuously differentiable function that maps $\Omega_\rho \to \Omega_{\frac{1}{2}}$, strictly increasing and invertible [2].

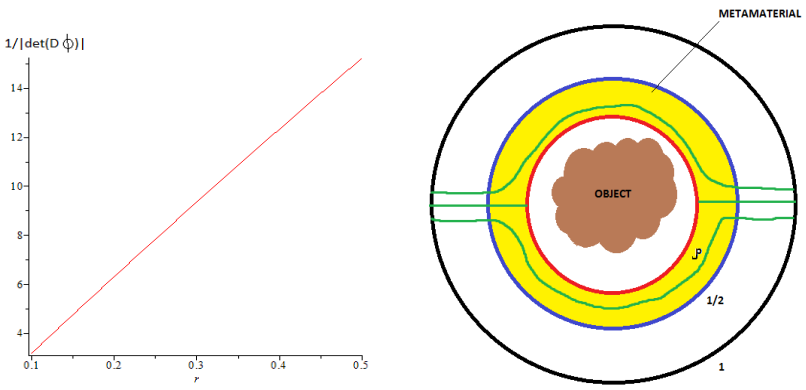

Figure 8: *This is a plot of* $\frac{1}{|\det(D\Phi)|}$ *versus* r *in the yellow cloaking region* $\rho \leq r \leq \frac{1}{2}$*, where* $\rho = 0.10$ *and* $\delta = 0.05$.

Choose $\Psi(r) = \frac{1}{2} + \frac{\delta}{1-2\rho}(r-\rho)$ for the cloaking region $\rho \leq r \leq \frac{1}{2}$ that we are interested in examining, with $\rho = 0.10$ and $\delta = 0.05$. We generate the following plot of $\frac{1}{|\det(D\Phi)|}$ versus r. The generated plot in Figure 8 provides a meaningful interpretation to the physical property in the cloaking region. In the inner boundary, there is low thermal conductivity as shown by the lower values of $\frac{1}{|\det(D\Phi)|}$ as r becomes smaller. In the area near the metamaterial, there is high thermal conductivity as noted by the increasing value of $\frac{1}{|\det(D\Phi)|}$. This gives information about the properties needed in the anisotropic conductivity for the metamaterial.

We've now shown how one can design an anisotropic layer to make a hole of radius $1/2$ appear as a hole of radius ρ to an observer using the heat equation at fixed frequency ω. It's worth noting that the anisotropic conductivity σ required (as well as the altered density/specific heat) do not depend on the imaging frequency ω. However, we must now show that a region with a hole of radius $\rho \approx 0$ looks like a region with no hole at all, by showing the relevant boundary data on $\partial\Omega_0$ are close.

4 Estimation of the Cloak Efficiency

To surpass the outside observer's ability to detect the hidden object, the difference in the temperature w_0 on the unit disk versus the temperature w_ρ on the annulus needs to be sufficiently small. We will prove that this is the case, that if an observer inputs Neumann data g into the disk Ω_0 with no hole (so $\frac{\partial w_0}{\partial n} = g$) and then into the annulus with hold of radius ρ ($\frac{\partial w_\rho}{\partial n} = g$) we will have $\|w_\rho - w_0\|_{L^2(\partial\Omega_0)} \to 0$ as $\rho \to 0^+$. One method to do so is to use modern ideas from partial differential equations: *trace estimates*. The trace of a function is essentially the value of the function on just the boundary of the domain. In what follows we will assume the functions w_ρ and w_0 are twice continuously differentiable on $\bar{\Omega}$ (the closure of Ω).

Let $\phi(x, y)$ be a C^2 function defined on a region B in $\mathbb{R}^2$ (with ϕ continuous on $\bar{B}$). If S

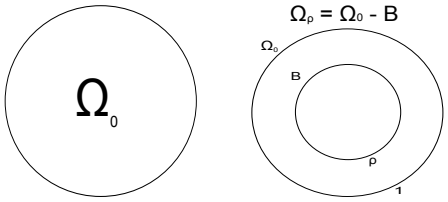

is an portion of ∂B we define

$$\|\phi\|_{L^2(S)} := \left(\int_S \phi^2 \, ds \right)^{1/2}$$

where ds denotes arc length. We will show that

Lemma 3 *We have the inequality* $\|w_\rho - w_0\|_{L^2(r=1)} \leq C\sqrt{\rho}$ *for some constant* C *that does not depend on* ρ.

In short, the difference between w_ρ and w_0, as measured in the L^2 norm, can be made as small as we like by taking ρ sufficiently small. Since the cloaked hole of radius $1/2$ can be made indistinguishable from Ω_ρ, we can cloak to any desired degree of accuracy by taking ρ sufficiently small.

The rest of this section provides a proof to Lemma 3. We start with two preliminary lemmas.

Lemma 4 *We have*

$$\left\| \frac{\partial w_0}{\partial n} \right\|_{L^2(r=\rho)} \leq C\sqrt{\rho} \tag{26}$$

for some constant C *that does not depend on* ρ.

Proof: To prove this lemma we parameterize the curve $r = \rho$ as

$$x = \rho\cos(\theta), \quad y = \rho\sin(\theta)$$

with $0 \leq \theta \leq 2\pi$. Note then that $ds = \rho \, d\theta$.

By definition, $\frac{\partial w_0}{\partial n} = \nabla w_0 \cdot n =< \frac{\partial w_0}{\partial x}, \frac{\partial w_0}{\partial y} > \cdot < -\rho\cos\theta, -\rho\sin\theta >$ (since n points toward the origin, i.e., out of Ω_ρ.) Then equation (26 can be expressed as

$$\left\| \frac{\partial w_0}{\partial n} \right\|^2_{L^2(r=\rho)} = \rho \int_0^{2\pi} \left(\frac{\partial w_0}{\partial x}\cos\theta + \frac{\partial w_0}{\partial y}\sin\theta \right)^2 d\theta \tag{27}$$

From the inequality $(a+b)^2 \leq 2a^2 + 2b^2$ we then have

$$\left\| \frac{\partial w_0}{\partial n} \right\|^2_{L^2(r=\rho)} \leq 2\rho \int_0^{2\pi} \left[\left(\frac{\partial w_0}{\partial x} \right)^2 \cos^2(\theta) + \left(\frac{\partial w_0}{\partial y} \right)^2 \sin^2(\theta) \right] d\theta. \tag{28}$$

Since Ω_0 is a compact set, and we assume w_0 bounded and continuously differentiable on Ω, we see that $\frac{\partial w_0}{\partial x} \leq M$ and $\frac{\partial w_0}{\partial y} \leq K$ on Ω for some constants K, M. From equation (28) we can then bound

$$\left\| \frac{\partial w_0}{\partial n} \right\|^2_{L^2(r=\rho)} \leq 2\rho \int_0^{2\pi} (M^2 \cos^2(\theta) + K^2 \sin^2(\theta))\, d\theta. \tag{29}$$

Evaluating the right side of (29) yields

$$\left\| \frac{\partial w_0}{\partial n} \right\|^2_{L^2(r=\rho)} \leq 2\pi\rho(M^2 + K^2). \tag{30}$$

This shows that (26) holds with $C = \sqrt{2\pi(M^2 + K^2)}$, which is independent of ρ. This completes the proof of Lemma 4.

We now use the estimate (26) to show that the quantity $\|w - w_0\|_{L^2(r=1)} \to 0$ as $\rho \to 0$. The technique use is that of *trace estimates* for the quantity $w - w_0$.

Recall that the function w_0 satisfies $\Delta w_0 - i\omega w_0 = 0$ in Ω_0 with Neumman data $\frac{\partial w_0}{\partial n} = g$. The function w_ρ satisfies $\Delta w_\rho - i\omega w_\rho = 0$ in Ω_ρ with Neumman data $\frac{\partial w_0}{\partial n} = g$ on the outer boundary $r = 1$ and $\frac{\partial w_0}{\partial n} = 0$ on $r = \rho$. Define $v_\rho = w_0 - w_\rho$ to be the difference between the solutions on the annulus Ω_ρ. Then

$$\Delta v_\rho - i\omega v_\rho = 0 \text{ in } \Omega_\rho \tag{31}$$

with boundary conditions

$$\frac{\partial v_\rho}{\partial n} = 0 \text{ on } r = 1 \tag{32}$$

$$\frac{\partial v_\rho}{\partial n} = -\frac{\partial w_0}{\partial n} \text{ on } r = \rho. \tag{33}$$

Recall that the H^1 Sobolev norm for a function ϕ over a region $D \subset \mathbb{R}^2$ is

$$\|v\|_{H^1(D)} := \left(\int_D (|\phi|^2 + |\nabla\phi|^2) dx \right)^{\frac{1}{2}}. \tag{34}$$

Lemma 5 *We have the trace inequalities*

$$\|v\|_{L^2(r=\rho)} \leq C\|v\|_{H^1(\Omega_\rho)} \tag{35}$$

and

$$\|v\|_{L^2(r=1)} \leq C\|v\|_{H^1(\Omega_\rho)} \tag{36}$$

for some constant C that does not depend on ρ.

Proof: Let us focus in (35). First, in polar coordinates with $v = v(r,\theta)$ we have

$$\|v\|_{L^2(r=\rho)} = \sqrt{\int_0^{2\pi} |v(\rho,\theta)|^2 \rho d\theta}. \tag{37}$$

Similarly

$$\begin{aligned} ||v||_{H^1(\Omega_\rho)} &= \int_0^{2\pi}\int_\rho^1 \left(|v(r,\theta)|^2 + |\nabla v(r,\theta)|^2\right) r dr\, d\theta \\ &= \int_0^{2\pi}\int_\rho^1 \left(|v(r,\theta)|^2 + |v_r|^2 + |v_\theta|^2/r^2\right) r dr\, d\theta \end{aligned} \tag{38}$$

using the fact that in polar coordinates $|\nabla v|^2 = |v_r|^2 + |v_\theta|^2/r^2$.

Now note that

$$v(r,\theta) - v(\rho,\theta) = \int_\rho^r v_r(t,\theta) dt$$

for and $\rho < r < 1$. Take the absolute value of both sides of the above to obtain

$$\begin{aligned} |v(r,\theta) - v(\rho,\theta)| &= \left|\int_\rho^r v_r(t,\theta) dt\right| \\ &\leq \int_\rho^r |v_r(t,\theta)| dt \\ &\leq \left(\int_\rho^r 1^2 dr\right)^{\frac{1}{2}} \left(\int_\rho^r |v_r(t,\theta)|^2 dt\right)^{\frac{1}{2}} \\ &\leq \sqrt{r-\rho}\left(\int_\rho^r |v_r(t,\theta)|^2\right)^{\frac{1}{2}}. \end{aligned} \tag{39}$$

Using the reverse triangle inequality $|v(\rho,\theta)| - |v(r,\theta)| \leq |v(\rho,\theta) - v(r,\theta)|$ yields

$$|v(\rho,\theta)| - |v(r,\theta)| \leq \sqrt{r-\rho}\left(\int_\rho^r |v_r(t,\theta)|^2 dt\right)^{\frac{1}{2}}$$

or

$$|v(\rho,\theta)| \leq |v(r,\theta)| + \sqrt{r-\rho}\left(\int_\rho^r |v_r(t,\theta)|^2 dt\right)^{\frac{1}{2}}.$$

We next square both sides of the inequality above and apply the inequality $(|a|+|b|)^2 \leq 2|a|^2 + 2|b|^2$ to obtain

$$|v(\rho,\theta)|^2 \leq 2|v(r,\theta)|^2 + 2(r-\rho)\int_\rho^r |v_r(t,\theta)|^2 dt.$$

Integrating the above from $\theta = 0$ to $r = 2\pi$ and multiplying through by ρ yields

$$\begin{aligned} \int_0^{2\pi} |v(\rho,\theta)|^2 \rho d\theta &\leq 2\int_0^{2\pi} |v(r,\theta)|^2 \rho d\theta + 2(r-\rho)\int_0^{2\pi}\int_\rho^r |v_r(t,\theta)|^2 \rho dt \\ &\leq 2\int_0^{2\pi} |v(r,\theta)|^2 r d\theta + 2(r-\rho)\int_0^{2\pi}\int_\rho^r |v_r(t,\theta)|^2 t dt \end{aligned}$$

since $\rho < r$ (and $\rho < t$ in the last integrand). This last inequality yields (use the fact that $r < 1$ in the last integral)

$$\int_0^{2\pi} |v(\rho,\theta)|^2 \rho d\theta \leq 2\int_0^{2\pi} |v(r,\theta)|^2 r d\theta + 2(r-\rho)\int_0^{2\pi}\int_\rho^1 |v_r(t,\theta)|^2 t dt$$

or

$$\|v\|^2_{L^2(r=\rho)} \leq 2\int_0^{2\pi} |v(r,\theta)|^2 r d\theta + 2(r-\rho)\|v_r\|^2_{L^2(\Omega_\rho)}.$$

Integrate both sides above in r from $r = \rho$ to $r = 1$ and divide by $1-\rho$ to find

$$\|v\|^2_{L^2(r=\rho)} \leq \frac{2}{1-\rho}\int_\rho^1\int_0^{2\pi} |v(r,\theta)|^2 r\, dr\, d\theta + \|v_r\|^2_{L^2(\Omega_\rho)}.$$

This immediately yields (35), in light of (38).

The inequality (36) can be shown similarly.

To complete the proof of Lemma 4), multiply both sides of (31) by $\bar{v}$, integrate over Ω_ρ, and apply the Divergence Theorem with the boundary conditions (32) and (33), to obtain

$$\int_{\Omega_\rho} |\nabla v_\rho|^2\, dA + i\omega\int_{\Omega_\rho} |v|^2\, dA = -\int_{r=\rho} \bar{v}\frac{\partial w_0}{\partial n}\, ds. \tag{40}$$

The right side of (40) can be bounded via the Cauchy-Schwarz inequality, as

$$\left| -\int_{r=\rho} \bar{v}\frac{\partial w_0}{\partial n}\, ds \right| \leq \|v\|_{L^2(r=\rho)}\|\partial w_0/\partial n\|_{L^2(\rho)} \leq C\sqrt{\rho}\|v\|_{L^2(r=\rho)} \tag{41}$$

where the last inequality follows from (26). The left side of (40) can be bounded below by using the elementary fact that $a + b \leq (1 + 1/\omega)|a + i\omega b|$ for $a, b > 0$ and yields

$$\|v_\rho\|^2_{H^1(\Omega_\rho)} \leq (1+1/\omega)\left(\int_{\Omega_\rho} |\nabla v_\rho|^2\, dA + i\omega\int_{\Omega_\rho} |v|^2\, dA\right) \tag{42}$$

If we combine (42), (40), and (41) we have

$$\|v_\rho\|^2_{H^1(\Omega_\rho)} \leq C(1+1/\omega)\sqrt{\rho}\|v\|_{L^2(r=\rho)}. \tag{43}$$

With (35) we then obtain

$$\|v_\rho\|^2_{H^1(\Omega_\rho)} \leq C(1+1/\omega)\sqrt{\rho}\|v_\rho\|_{H^1(\Omega_\rho)} \tag{44}$$

Which yields the bound

$$\|v_\rho\|_{H^1(\Omega_\rho)} \leq C(1+1/\omega)\sqrt{\rho}. \tag{45}$$

Finally, application of (36) yields

$$\|v_\rho\|_{L^2(r=1)} \leq C(1+1/\omega)\sqrt{\rho}$$

which is the assertion of the lemma.

We have shown that $\|v\|_{L^2(r=1)} \leq C\sqrt{\rho}$. This means that the difference between the solutions on the unit disk and the annulus tends to zero as $\rho \to 0$. Thus by choosing ρ suitably small we can make w and w_0 as close as we like on the outer boundary $r = 1$.

5 Discussion

Through the change-of-variables argument and the use of trace estimates, we showed that it is possible to cloak against thermal imaging. In the change-of-variables argument, we showed that we can make a large hole to appear small by surrounding it with a layer of metamaterial. The physical interpretations in the argument indicates that in the cloaking region, as r approaches $\frac{1}{2}$, there will be higher thermal conductivity. This makes sense because as the metamaterial bends the heat around the hidden object, the heat gets pinched around the region near the metamaterial. The use of trace estimates shows that the difference between the solutions on the unit disk and the annulus is bounded by $\sqrt{\rho}$. If ρ is close to zero, then the difference between the solutions is also close to zero. For future work, a careful manipulation in algebra may bound the difference between the two solutions by ρ^2 instead of $\sqrt{\rho}$. Thus, we have proved mathematically that cloaking against thermal imaging can be done similarly as cloaking against electrical impedance tomography.

References

[1] Abramowitz, Milton and Stegun, Irene A., *Handbook of Mathematical Functions*, Dover Publications, New York, 1972.

[2] Bryan, Kurt and Leise, Tanya, *Impedance Imaging, Inverse Problems, and Harry Potter's Cloak*, in SIAM Review, Vol. 52, No. 2, pp. 359-377.

[3] Strauss, W., *Partial Differential Equations: An Introduction*, John Wiley & Sons, New York, 1992.

[4] Watson, G.N., *A Treatise on the Theory of Bessel Functions*, Merchant Books, 2008.

[5] Weisstein, Eric W. "Modified Bessel Differential Equation." From MathWorld–A Wolfram Web Resource.
http://mathworld.wolfram.com/ModifiedBesselDifferentialEquation.html